

Increased Heat Transport in Ultra-Hot Jupiter Atmospheres Through H₂ Dissociation/Recombination

TAYLOR J. BELL^{1,*} AND NICOLAS B. COWAN^{1,2,*}

¹*Department of Physics, McGill University, 3600 rue University, Montréal, QC H3A 2T8, Canada*

²*Department of Earth & Planetary Sciences, McGill University, 3450 rue University, Montréal, QC H3A 0E8, Canada*

(Received 2018 January 30)

Submitted to ApJL

ABSTRACT

A new class of exoplanets is beginning to emerge: planets whose dayside atmospheres more closely resemble stellar atmospheres as most of their molecular constituents dissociate. The effects of the dissociation of these species will be varied and must be carefully accounted for. Here we take the first steps towards understanding the thermodynamical consequences of dissociation and recombination of molecular hydrogen (H₂). Using a simple energy balance model with eastward winds, we demonstrate that H₂ dissociation/recombination can significantly increase the day–night heat transport on ultra-hot Jupiters: gas giant exoplanets where the temperature is $\gtrsim 2200$ K somewhere on the planet. For these planets, significant H₂ dissociation should occur on their highly irradiated daysides, transporting some of the energy deposited on the dayside towards the nightside of the planet where the H atoms recombine into H₂; this mechanism bears similarities to latent heat. Given a fixed wind speed, this will act to increase the heat recirculation efficiency; alternatively, a measured heat recirculation efficiency will require slower wind speeds after accounting for H₂ dissociation/recombination.

Keywords: planets and satellites: atmospheres — planets and satellites: gaseous planets — methods: analytical — methods: numerical

1. INTRODUCTION

Most gas giant exoplanets have atmospheres dominated by molecular hydrogen (H₂). However, on planets where the temperature is $\gtrsim 2200$ K somewhere a significant fraction of the H₂ will thermally dissociate (Langmuir 1912); one may call these planets ultra-hot Jupiters (UHJs), rather than just hot Jupiters. Only a handful of known planets have dayside temperatures this high, but the TESS mission is expected to discover ~ 1500 more as it includes many early-type stars (George Zhou, private communication 2017). These UHJs are an interesting intermediate between stars and cooler planets, and they will allow for useful tests of atmospheric models.

Corresponding author: Taylor J. Bell
 taylor.bell@mail.mcgill.ca

* McGill Space Institute; Institute for Research on Exoplanets;
 Centre for Research in Astrophysics of Quebec

At these star-like temperatures, the H⁺ bound-free and free-free opacities should play an important role in the continuum atmospheric opacity which has recently been detected in dayside secondary eclipse spectra (Bell et al. 2017; Arcangeli et al. 2018). These recently reported detections of H⁺ opacity provide evidence that H₂ is dissociating in the atmospheres of gas giants at this temperature range. However, the thermodynamical effects of H₂ dissociation/recombination have yet to be explored.

Both theoretically (e.g. Perez-Becker & Showman 2013; Komacek & Showman 2016) and empirically (e.g. Zhang et al. 2018; Schwartz et al. 2017), we expect the day–night temperature contrast on hot Jupiters to increase with increasing stellar irradiation; temperature gradients $\gtrsim 1000$ K can be expected for UHJs. As temperatures vary drastically between day and night, the local thermal equilibrium (LTE) H₂ dissociation fraction will also vary. The recombination of H into H₂ is a remarkably exothermic process, releasing

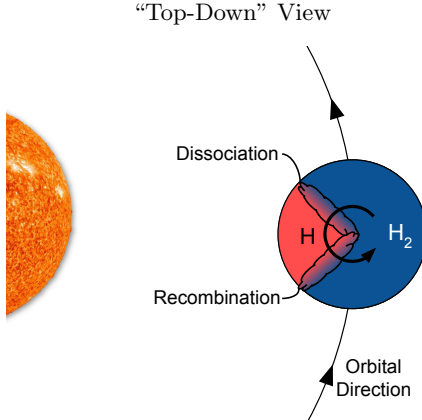


Figure 1. A cartoon showing a “top-down” view of the expected dissociation and recombination of H_2 on an ultra-hot Jupiter (UHJ). The orbital direction and the direction of winds on the planet are indicated with black arrows.

$q = 2.14 \times 10^8 \text{ J kg}^{-1}$; this is $100 \times$ more potent than the latent heat of condensation for water. For reference, latent heat is responsible for approximately half of the heat recirculation on Earth ($L/(c_p \Delta T) \sim 1$), while the effect of H_2 dissociation/recombination should be even stronger for UHJs ($q/(c_p \Delta T) \sim 10^2$). One can gain some intuition from this rough analogy.

Building on this intuition, we might expect that H will recombine into H_2 as gas carried by winds flows eastward from the sub-stellar point, significantly heating the eastern hemisphere of the planet. As the gas continues to flow around to the dayside, the H_2 will again dissociate and significantly cool the western hemisphere. A cartoon depicting this layout is shown in Figure 1. If unaccounted for while modelling a phasecurve, this would likely manifest itself as an “unphysically” large eastward offset as was previously reported for WASP-12b (Cowan et al. 2012).

A large number of circulation models have been developed for studying exoplanet atmospheres, ranging from simple energy balance models (e.g. Cowan & Agol 2011) to more advanced general circulation models (e.g. Showman et al. 2009; Rauscher & Menou 2010; Amundsen et al. 2014; Zhang & Showman 2017; Heng & Kitzmann 2017; Dobbs-Dixon & Cowan 2017). To our knowledge, however, no atmospheric models published so far include a heating/cooling term accounting for the energy released/absorbed by H_2 recombination/dissociation. Here we aim to qualitatively explore these effects using a simple energy balance model adapted from that described by Cowan & Agol (2011), using code based on that implemented by Schwartz et al. (2017). We leave it to those with more advanced circulation

models to explore this problem in a more rigorous and quantitative manner.

2. ENERGY TRANSPORT MODEL

2.1. Heating Terms

First, let ϵ be the energy per unit area of a parcel of gas. Ignoring H_2 dissociation/recombination and any internal heat sources, and assuming the gas parcel cools radiatively, energy conservation gives

$$\frac{d\epsilon}{dt} = F_{\text{in}} - F_{\text{out}},$$

with F_{in} and F_{out} given by

$$F_{\text{in}} = (1 - A_B)F_*(t) \sin \theta \max(\cos \Phi(t), 0),$$

$$F_{\text{out}} = \sigma T^4.$$

The planet’s Bond albedo is given by A_B , θ is the colatitude of the gas parcel, $\Phi(t)$ is the stellar hour angle, T is the temperature of the gas parcel, and σ is the Stefan-Boltzmann constant. The incoming stellar flux is given by $F_* = \sigma T_{*,\text{eff}}^4 (R_*/a)^2$, where $T_{*,\text{eff}}$ is the stellar effective temperature, R_* is the stellar radius, and a is the planet’s semi-major axis. The $\Phi(t)$ term incorporates both advection and planetary rotation.

In order to include H_2 dissociation/recombination, we must add a new term accounting for the energy flux due to these effects. This can be done with

$$\frac{d\epsilon}{dt} = F_{\text{in}} - F_{\text{out}} - \frac{d\mathbb{Q}}{dt}, \quad (1)$$

where the energy per unit area stored by H_2 dissociation is given by

$$\mathbb{Q} = q\chi\Sigma,$$

where Σ is the mass per unit area of H and H_2 in the parcel of gas (in kg m^{-2}), $q = 2.14 \times 10^8 \text{ J kg}^{-1}$ is the H_2 bond dissociation energy per unit mass at 0 K, and χ is the dissociation fraction of the gas. $\chi = 1$ means the gas is completely dissociated (all H). Assuming the gas parcel is in hydrostatic equilibrium, we can use

$$\Sigma = \int_{z_0}^{\infty} \rho(z) dz = (P_0/g)$$

where z_0 is some reference height, P_0 is the atmospheric pressure corresponding to z_0 , and ρ is the density of the gas. This then allows us to rewrite \mathbb{Q} as

$$\mathbb{Q} = (P_0/g)q\chi.$$

The time derivative of \mathbb{Q} is then

$$\frac{d\mathbb{Q}}{dt} = (P_0/g)q \frac{d\chi}{dt} = (P_0/g)q \frac{d\chi}{dT} \bigg|_T \frac{dT}{dt}, \quad (2)$$

where we have assumed the gas parcel's P_0/g remains constant, and where we have made use of the chain rule to expand $d\chi/dt$.

We model the LTE H₂ dissociation fraction using the equation given by Langmuir (1912):

$$\chi(P, T) = \frac{P_{\text{H}}}{P} = \frac{1}{2P} \left(-Y + \sqrt{Y^2 + 4PY} \right), \quad (3)$$

where

$$Y = 100^{-a+b/T} T,$$

and where P_{H} is the partial pressure of H (in atm), P is the total pressure (in atm), T is the temperature of the gas (in K), $a = 2.665$, and $b = 14400$. The LTE dissociation fraction is plotted in the top panel of Figure 2.

We can then find $d\chi/dT$ using the chain rule:

$$\frac{d\chi}{dT} = \frac{d\chi}{dY} \frac{dY}{dT}.$$

After some simplification, we then determine

$$\frac{d\chi}{dT} = (T^{-1} + b \ln 100T^{-2}) \left(\chi - \frac{Y}{\sqrt{Y^2 + 4PY}} \right). \quad (4)$$

To a good degree of accuracy, Equations (3) and (4) can be approximated at $P = 0.1$ bar using

$$\chi(0.1 \text{ bar}, T) = \frac{1}{2} \left(1 + \text{erf} \left(\frac{T - \mu}{\sigma\sqrt{2}} \right) \right) \quad (5)$$

and

$$\frac{d\chi(0.1 \text{ bar}, T)}{dT} = \frac{1}{\sigma\sqrt{2\pi}} e^{-(T-\mu)^2/2\sigma^2} \quad (6)$$

where $\sigma = 281$ K and $\mu = 2850$ K; this approximation offers a 20% increase in computation speed.¹ It should be noted that we assume that this H₂ dissociation/recombination occurs instantaneously since the timescale in the temperature regime of UHJs at 0.1 bar is $\sim 10^{-3}$ s (Rink 1962; Shui 1973).

2.2. Thermal Energy

We assume that the planet's energy is stored entirely as thermal energy (ignoring other terms, such as $P dV$ work), as is done in other simple energy balance models (e.g. Cowan & Agol 2011; Pierrehumbert 2010). This assumption means

$$\begin{aligned} \frac{d\epsilon}{dt} &= \frac{d}{dt} (c_p T \Sigma) = \frac{d}{dt} \left((P_0/g) c_p T \right) \\ &= (P_0/g) \left(c_p \frac{dT}{dt} + T \frac{dc_p}{dT} \right) \\ &= (P_0/g) \frac{dT}{dt} \left(c_p + T \frac{dc_p}{dT} \right). \end{aligned} \quad (7)$$

¹ Variations in these constants as a function of pressure are fairly simple to compute, requiring one to numerically solve the Lambert-W function at each desired pressure level.

where we have again assumed the gas parcel's P_0/g remains constant and have used the chain rule to expand dc_p/dt .

The heat capacity of the gas will change as a function of temperature due to the slightly different heat capacities of H and H₂ as well as the variations in the heat capacity of H₂ as a function of temperature (Chase 1998). Any model properly accounting for H₂ dissociation should account for this effect. In our model, we model this by assuming the gas is well mixed so that

$$c_p = c_{p,\text{H}} \chi + c_{p,\text{H}_2} (1 - \chi),$$

where both χ and c_{p,H_2} are functions of temperature. The temperature derivative of c_p is then given by

$$\frac{dc_p}{dT} \Big|_T = (c_{p,\text{H}} - c_{p,\text{H}_2}) \frac{d\chi}{dT} \Big|_T + \frac{dc_{p,\text{H}_2}}{dT} \Big|_T (1 - \chi).$$

2.3. Putting Everything Together

Putting together Equations (1), (2) and (7), we get

$$\begin{aligned} F_{\text{in}} - F_{\text{out}} - (P_0/g) \frac{dT}{dt} \left(q \frac{d\chi}{dT} \Big|_T \right) \\ = (P_0/g) \frac{dT}{dt} \left(c_p + T \frac{dc_p}{dT} \Big|_T \right). \end{aligned}$$

After solving for dT/dt , we find

$$\frac{dT}{dt} = (F_{\text{in}} - F_{\text{out}})(P_0/g)^{-1} \left(c_p + T \frac{dc_p}{dT} \Big|_T + q \frac{d\chi}{dT} \Big|_T \right)^{-1}.$$

Finally, a gas cell can then be updated using

$$\Delta T = \frac{\Delta t (F_{\text{in}} - F_{\text{out}})}{(P_0/g) \left(c_p + T \frac{dc_p}{dT} \Big|_T + q \frac{d\chi}{dT} \Big|_T \right)}. \quad (8)$$

3. SIMULATED OBSERVATIONS AND QUALITATIVE TRENDS

We now explore the effects of the new term in the differential equation governing the temperature of a gas cell. For this purpose, we create a 2D (latitude+longitude) HEALPix grid where each parcel's temperature is updated using Equation (8) with code based on that developed by Schwartz et al. (2017).

While Cowan & Agol (2011) were able to explore their model using dimensionless quantities, our updated model requires that we use dimensioned variables. We therefore adopt the values of the first discovered UHJ, WASP-12b (Hebb et al. 2009). In particular, we set $R_p = 1.90 R_J$, $a = 0.0234$ AU, $M_p = 1.470 M_J$, $T_{*,\text{eff}} = 6360$ K, $R_* = 1.657 R_\odot$, $P = 1.0914203$ days

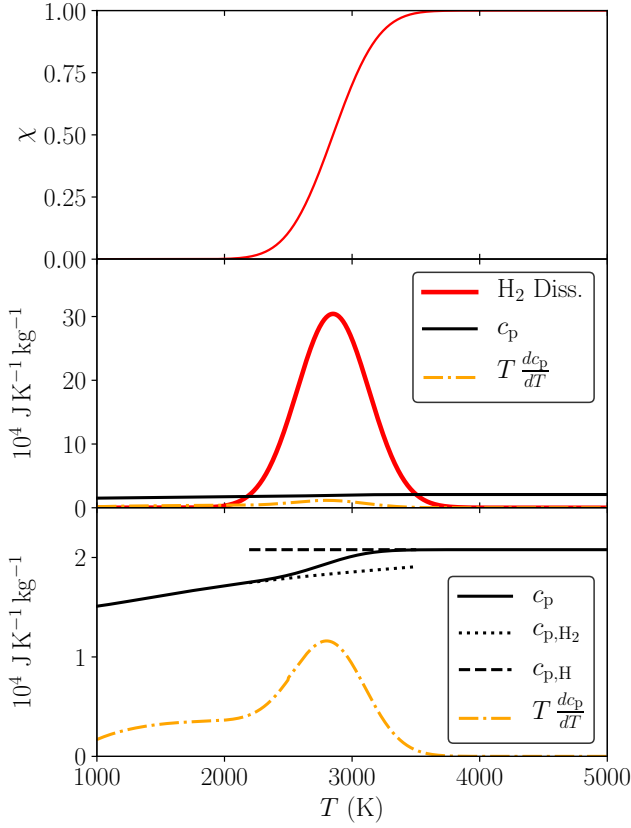


Figure 2. *Top:* The LTE dissociation fraction of H₂ in a parcel of gas. *Middle:* A demonstration of the relative importance of the H₂ dissociation/recombination term in Equation (8). For $T \gtrsim 2200$, the energy absorbed by H₂ dissociation is greater than the energy stored as heat. Typical hot Jupiters have temperatures around 1500 K and shouldn't be affected by H₂ dissociation/recombination, but these processes should dominate the heat capacity of UHJs. *Bottom:* An inset showing the specific heat capacity of a gas composed of H and H₂ in LTE (the same black line from the middle panel), as well as the specific heat capacities of H and H₂ where they are able to exist in equilibrium. The remaining $T(dc_p/dT)$ term is also shown.

(Collins et al. 2017) and $A_B = 0.27$ (Schwartz et al. 2017). We have also assumed a photospheric pressure of 0.1 bar (the approximate pressure probed by NIR observations of WASP-12b; (Stevenson et al. 2014)). Given these parameters, the expected radiative timescale for the substellar point of WASP-12b, assuming $A_B = 0$, is ~ 4 hours (similar to observed timescales for eccentric hot Jupiters, e.g. Lewis et al. 2013; de Wit et al. 2016). Wind speeds for WASP-12b have not been directly measured, but typical values for hot Jupiters are on the order of 1 km s⁻¹ (e.g. Koll & Komacek 2017); for that reason, we will focus on wind speeds around this order of magnitude.

First, let's explore the effects of H₂ dissociation/recombination at a spatially resolved scale. Figure 3 shows temperature and H₂ dissociation maps for three different wind speeds. In the limit of infinite wind speeds, there will be no temperature gradients and H₂ dissociation/recombination will not play a role; wind speeds > 10 km s⁻¹ begin to approach this limit. In the limit of an atmosphere in radiative equilibrium, there will be no variation in the temperature of a parcel and H₂ dissociation/recombination will play no role; wind speeds < 0.1 km s⁻¹ begin to approach this limit. Outside of these two unphysical limits, H₂ dissociation/recombination will always be occurring somewhere on UHJs.

We now zoom out to disk integrated observations in order to see the effects on phascurve observations. This requires that we convolve the planet map, M , with a visibility kernel, K , at each orbital phase, ψ , (Cowan et al. 2013):

$$F_{\text{obs}}(\psi) = \oint K(\Omega, \psi) M(\Omega, \psi) d\Omega$$

where $\oint d\Omega$ is the integral over the planet's surface; this acts as a low-pass filter. Figure 4 shows model phascurves for the same three wind speeds as in Figure 3. It is clear that H₂ dissociation/recombination can have a strong effect, even on a fairly cool UHJ like WASP-12b. At a constant wind speed, the first obviously affected observable is the increased offset of the peak in the phascurve towards the east (the same direction as the prescribed wind). Another affected observable is the amplitude of the phase variations which is reduced when H₂ dissociation/recombination is included.

Figure 5 demonstrates the changes in these two observables for a wide range of wind speeds, with models sharing a wind speed connected by a line. Our model suggests that H₂ dissociation/recombination always affects the phase offset, while it only decreases temperature contrast for sufficiently strong wind speeds. Also, a Fourier decomposition shows that nearly all of the power in the phascurves accounting for H₂ dissociation/recombination is in the first and second order Fourier series terms ($f = 1f_{\text{orb}}$ or $2f_{\text{orb}}$) which may make these effects difficult to distinguish from increased wind speed and tidal distortion of the planet.

4. MODEL ASSUMPTIONS

With simplistic models, many important effects are necessarily swept under the rug. Here we aim to lift up the rug and shine a light on our assumptions so as to aid future work. While many of these assumptions will change the quantitative effects of H₂ dissociation/

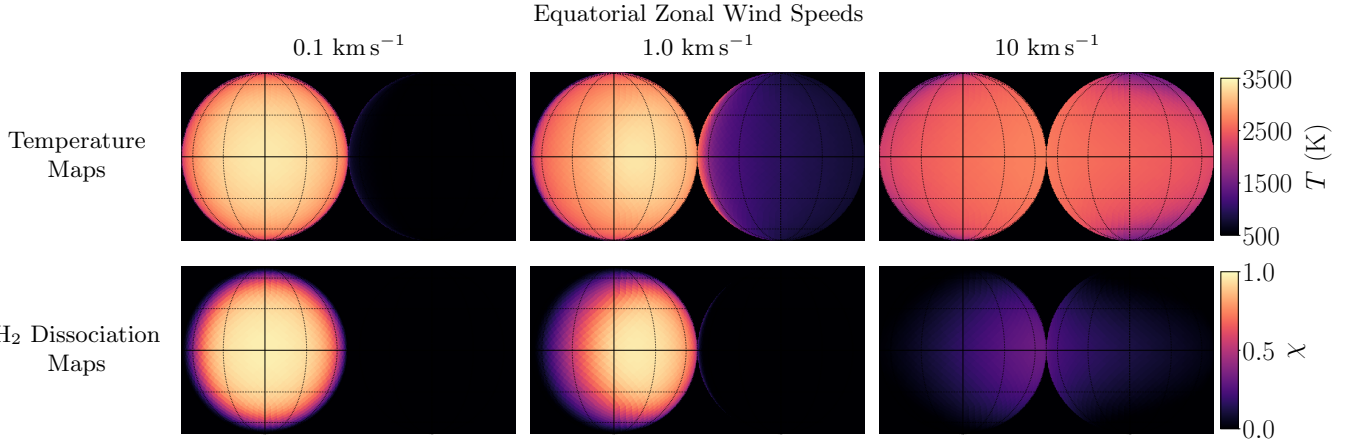


Figure 3. Planetary maps, showing temperature and H₂ dissociation fraction, assuming different eastward zonal wind speeds. The dayside hemisphere is shown on the left side of each map with north at the top.

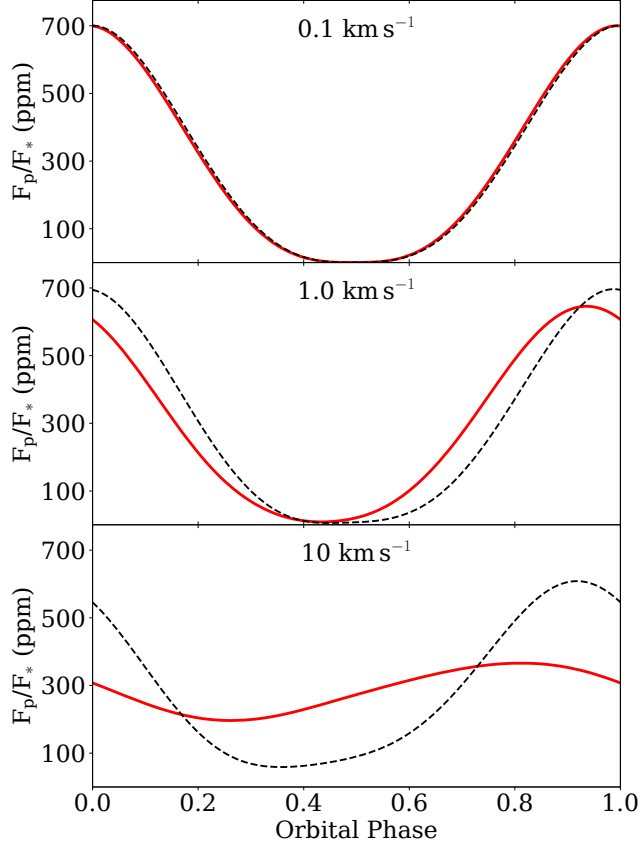


Figure 4. Model *bolometric* phasewcurves assuming different eastward zonal wind velocities, ignoring eclipses and transits. The red line shows the expected phasewcurve accounting for H₂ dissociation/recombination, while the black, dashed model neglects these processes.

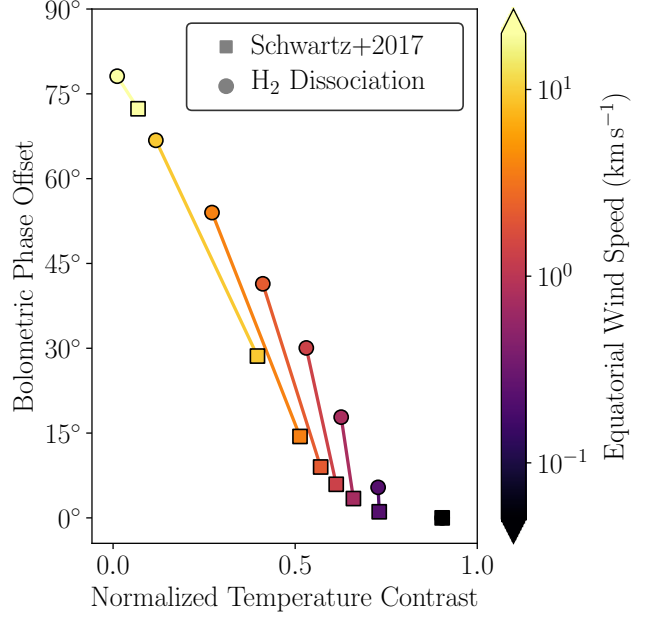


Figure 5. A figure showing the relationship between the offset in the peak of a phasewcurve and the normalized temperature contrast, given theoretical *bolometric* phasewcurve measurements. Normalized temperature contrast is computed using $(T_{\max} - T_{\min})/T_0$ where T_{\max} and T_{\min} are the maximum and minimum disk-integrated and visibility weighted temperatures, and $T_0 = T_{*,\text{eff}} \sqrt{R_*/a}$ is the planet's irradiation temperature. Circles show models including H₂ dissociation/recombination for WASP-12b, while squares show models neglecting these effects (selected points from Schwartz et al. 2017). Models sharing the same wind speed are connected by lines of the same colour.

recombination, we expect that the overall qualitative impact of increased heat recirculation will be robust to these assumptions.

One important piece of physics that we have ignored (beyond a simple assumption of a 0.1 bar photosphere) is atmospheric opacity. As Dobbs-Dixon & Cowan (2017) demonstrated, variations in opacity sources as a function of longitude can change the depth of the photosphere by an order of magnitude or more. Changing the H_2 dissociation fraction will change the importance of H^- as an opacity source, with H_2O , CO, and other standard opacity sources also likely playing a role towards the cooler nightside. The insignificant detection of H_2O on the dayside of WASP-12b (Stevenson et al. 2014) but detection in the planet’s transmission spectrum (Kreidberg et al. 2015) clearly demonstrates that opacity sources should be expected to change on UHJs. Several of these other molecular opacity sources will also overlap with the far broader H^- absorption, which complicates a definitive detection of H^- using broadband photometry, such as that from *Spitzer*. The formation of clouds on the nightside of the planet would further complicate the interpretation of observed phasecurves, increasing the albedo of the west terminator while also insulating the nightside. While we have accounted for variations in the radiative timescale as a function of temperature, we have not accounted for these changes due to varying opacity sources.

Additionally, as we have assumed all photons are emitted at a 0.1 bar photosphere, the effects of the atmosphere’s T-P profile have been neglected. As the H_2 dissociation fraction has a fairly weak dependence on gas pressure, the bulk of vertical variations in the H_2 dissociation fraction will likely be controlled by the vertical temperature gradient. Due to the lower density of the dissociated gas, one may expect this to cause vertical advection in the absence of a temperature inversion. Interestingly, however, observations of most UHJs are best explained by atmospheres with thermal inversions (Arcangeli et al. 2018; Evans et al. 2017) or at least approximately isothermal profiles on the dayside (Crossfield et al. 2012; Cowan et al. 2012). Any non-isothermal T-P profile will alter the specifics of how efficiently heat is redistributed across the planet as different vertical layers in a gas column will dissociate/recombine at different locations. Also, as we have neglected atmospheric opacity, we have assumed that the planet emits as a blackbody with a single temperature as opacity sources are the cause of deviations from a blackbody.

Further, due to the changing scale height of the atmosphere at different longitudes due to changes in temperature and H_2 dissociation fraction, there will likely be a

tendency for gas to flow away from the sub-stellar point both zonally and meridionally. This is not accounted for in our toy model and would require a general circulation model. Instead, we have chosen eastward winds as they are seen for most hot Jupiters (e.g. Showman & Guillot 2002; Zhang et al. 2018), although there are some exceptions (e.g. Dang et al. 2018). Similarly, our assumption of solid-body rotation without variations in wind speed as a function of latitude, longitude, altitude, or time is clearly an over simplification which will need to be addressed in future work. Our model is also unable to predict the wind speeds of UHJs which would require the implementation of various drag sources, such as magnetic drag which Koll & Komacek (2017) suggests will dominate for hot Jupiters with $T_{eq} > 1400$ K.

Also, we have assumed all heating is due to H_2 dissociation and radiation from the host star, neglecting other internal heat sources such as residual heat from formation (which should be negligible for planets older than 1 Gyr; Burrows et al. 2006) as well as tidal, viscous, and ohmic heating. Finally, we have assumed that the planet has a uniform albedo which will not be the case in general (e.g. Esteves et al. 2013; Demory et al. 2013; Angerhausen et al. 2015; Parmentier et al. 2016).

5. DISCUSSION AND CONCLUSIONS

A new class of exoplanets is beginning to emerge: planets whose dayside atmospheres resemble stellar atmospheres as their molecular constituents thermally dissociate. The impacts of this dissociation will be varied and must be carefully accounted for. Here we have shown that the dynamical dissociation and recombination of H_2 will play an important role in the heat recirculation of ultra-hot Jupiters. For planets whose atmospheres reach $\gtrsim 2200$ K, significant H_2 dissociation should occur, absorbing some of the energy deposited on the dayside and transporting it towards the nightside of the planet. Given a fixed wind speed, this will act to increase the heat recirculation efficiency; alternatively, a measured heat recirculation efficiency will require slower wind speeds once H_2 dissociation/recombination has been accounted for.

Both theoretically and observationally, it has been shown that increasing irradiation tends to lead to poorer heat recirculation (e.g. Komacek & Showman 2016; Schwartz et al. 2017). However, there are a few notable exceptions to this rule at the high temperatures. Recently, Zhang et al. (2018) reported a heat recirculation efficiency of $\varepsilon \sim 0.2$ for the UHJ WASP-33b which is far higher than would be predicted by theoretical and observational trends. WASP-12b may also possess an unusually high heat recirculation efficiency and

exhibit a greater phase offset than would be expected from simple heat advection² (Cowan et al. 2012). However, the power in the second order Fourier series terms from H₂ dissociation/recombination seems to make the phascurve more sharply peaked and does not seem to be able to explain the double-peaked phascurve seen for WASP-12b by Cowan et al. (2012); further observations are required to determine whether this characteristic is an artifact of *Spitzer* systematics. Also, while Arcangeli et al. (2018) find evidence of H₂ dissociation/recombination in the atmosphere of WASP-18b, Maxted et al. (2013) finds the planet has minimal day–night heat recirculation; this suggests that WASP-18b has very weak winds or is too cool for H₂ dissociation/recombination to play a strong role in the heat recirculation of this planet. Finally, *Spitzer* or *James*

Webb observations of KELT-9b, the hottest UHJ currently known (Gaudi et al. 2017), could provide a fantastic test of this theory in the very high temperature regime.

T.J.B. acknowledges support from the McGill Space Institute Graduate Fellowship and from the FRQNT through the Centre de recherche en astrophysique du Québec. The atmospheric model we use was based upon code originally developed by Diana Jovmir and Joel Schwartz. We also thank Ian Dobbs-Dixon for his helpful insights. We have also made use of free and open-source software provided by the Python, SciPy, and Matplotlib communities.

REFERENCES

Amundsen, D. S., Baraffe, I., Tremblin, P., et al. 2014, *A&A*, 564, A59

Angerhausen, D., DeLarme, E., & Morse, J. A. 2015, *PASP*, 127, 1113

Arcangeli, J., Desert, J.-M., Line, M. R., et al. 2018, *ArXiv e-prints*, arXiv:1801.02489

Bell, T. J., Nikolov, N., Cowan, N. B., et al. 2017, *ApJL*, 847, L2

Burrows, A., Sudarsky, D., & Hubeny, I. 2006, *ApJ*, 650, 1140

Chase, M. W. 1998, *J. Phys. Chem. Ref. Data, Monograph* 9, 1

Collins, K. A., Kielkopf, J. F., & Stassun, K. G. 2017, *AJ*, 153, 78

Cowan, N. B., & Agol, E. 2011, *ApJ*, 729, 54

Cowan, N. B., Fuentes, P. A., & Haggard, H. M. 2013, *MNRAS*, 434, 2465

Cowan, N. B., Machalek, P., Croll, B., et al. 2012, *ApJ*, 747, 82

Crossfield, I. J. M., Barman, T., Hansen, B. M. S., Tanaka, I., & Kodama, T. 2012, *ApJ*, 760, 140

Dang, L., Cowan, N. B., Schwartz, J. C., et al. 2018, *ArXiv e-prints*, arXiv:1801.06548

de Wit, J., Lewis, N. K., Langton, J., et al. 2016, *ApJL*, 820, L33

Demory, B.-O., de Wit, J., Lewis, N., et al. 2013, *ApJL*, 776, L25

Dobbs-Dixon, I., & Cowan, N. B. 2017, *ApJL*, 851, L26

Esteves, L. J., De Mooij, E. J. W., & Jayawardhana, R. 2013, *ApJ*, 772, 51

Evans, T. M., Sing, D. K., Kataria, T., et al. 2017, *Nature*, 548, 58

Gaudi, B. S., Stassun, K. G., Collins, K. A., et al. 2017, *Nature*, 546, 514

Hebb, L., Collier-Cameron, A., Loeillet, B., et al. 2009, *ApJ*, 693, 1920

Heng, K., & Kitzmann, D. 2017, *ApJS*, 232, 20

Koll, D. D. B., & Komacek, T. D. 2017, *ArXiv e-prints*, arXiv:1712.07643

Komacek, T. D., & Showman, A. P. 2016, *ApJ*, 821, 16

Kreidberg, L., Line, M. R., Bean, J. L., et al. 2015, *ApJ*, 814, 66

Langmuir, I. 1912, *Journal of the American Chemical Society*, 34, 860

Lewis, N. K., Knutson, H. A., Showman, A. P., et al. 2013, *ApJ*, 766, 95

Maxted, P. F. L., Anderson, D. R., Doyle, A. P., et al. 2013, *MNRAS*, 428, 2645

Parmentier, V., Fortney, J. J., Showman, A. P., Morley, C., & Marley, M. S. 2016, *ApJ*, 828, 22

Perez-Becker, D., & Showman, A. P. 2013, *ApJ*, 776, 134

Pierrehumbert, R. T. 2010, *Principles of Planetary Climate*

Rauscher, E., & Menou, K. 2010, *ApJ*, 714, 1334

Rink, J. P. 1962, *JChPh*, 36, 262

Schwartz, J. C., Kashner, Z., Jovmir, D., & Cowan, N. B. 2017, *ApJ*, 850, 154

² Depending on the decorrelation method used to reduce the *Spitzer*/IRAC data for WASP-12b, the planet either has $\varepsilon \sim 0$ or $\varepsilon \sim 0.5$ (Cowan et al. 2012; Schwartz et al. 2017); although the former is the preferred model, further observations are critical to definitively choose between these values and test the predictions made in this article.

Showman, A. P., Fortney, J. J., Lian, Y., et al. 2009, *ApJ*, 699, 564

Showman, A. P., & Guillot, T. 2002, *A&A*, 385, 166

Shui, V. H. 1973, *JChPh*, 58, 4868

Stevenson, K. B., Bean, J. L., Madhusudhan, N., & Harrington, J. 2014, *ApJ*, 791, 36

Zhang, M., Knutson, H. A., Kataria, T., et al. 2018, *AJ*, 155, 83

Zhang, X., & Showman, A. P. 2017, *ApJ*, 836, 73